Analysis of propagation in periodically loaded circular waveguides

S. Amari
R. Vahldieck
J. Bornemann

Abstract: A technique is presented for the analysis of propagation in a circular waveguide periodically loaded with irises of finite thickness. The propagation constants of the Floquet modes are determined from the classical eigenvalues of a characteristic matrix instead of a nonlinear determinant equation. Numerical results are presented for the TE_{0n} modes and compared with available data. Excellent agreement is documented.

1 Introduction

Corrugated waveguides have been extensively investigated for applications in radar and microwave communication systems, linear accelerators and slow-wave devices. Antenna feed systems often include corrugations to achieve high degrees of isotropy in the radiation pattern and low cross-polarisation [1].

Corrugated circular waveguides have been investigated using a number of techniques [1]. Expansions of the components of the electromagnetic field in space harmonics have been extensively used in investigating propagation properties of periodically loaded waveguides [2]. In the surface-impedance approach, it is assumed that only the TM_{n0} mode is present in the slot where no propagation occurs [1–4]. The surface-impedance approach provides accurate results for the propagation constant of the modes when the corrugations are densely packed. In addition, the thickness of the irises is often neglected to simplify the analysis [5].

The use of space harmonics to expand the components of the electromagnetic field introduces an additional sum due to the quantisation in the direction of propagation [1]. The resulting double sums are truncated in the actual numerical solution, leading to a homogeneous matrix equation in the expansion coefficients. The propagation constants of the Floquet modes are determined by solving a nonlinear determinant equation following an iterative process. Such an approach can be time-consuming when a large number of modes are required.

The modified residue calculus technique has also been used in investigating periodically loaded waveguides [6]. The method is, however, applicable only for certain modal configurations [7]. The propagation properties of a rectangular waveguide periodically loaded with zero-thickness capacitive irises have been investigated with the mode-matching technique (MMT) [8]. The periodicity condition of the Floquet modes was imposed on the modal expansion coefficients, along with the boundary conditions at the interface between two adjacent unit cells, to derive an eigenvalue equation for the propagation constant. Here we improve on the analysis of Collin [8] by including the edge condition and, most importantly, taking into account the finite thickness of the irises.

The formulation used in this paper is based on the coupled-integral-equation technique [9]. Although eigenvalue problems in planar transmission lines with a thick metallic coating have also been formulated in terms of the aperture electric fields [10, 11], resulting in a nonlinear determinant equation [[10], eqn. 24] for the propagation constant, here we are interested in determining the propagation constants from the classical eigenvalues of a matrix instead of a determinant. This is achieved by not including the propagation constants in the modes used to expand the fields in the different regions; the propagation constant of a generic Floquet mode is included as *a priori* information in the integral equation instead. Finally, the edge condition is included by introducing a weighting factor as in the discussion of Kitazawa *et al.* [10].

In this paper, we limit the analysis to TE_{0n} modes in order to not cloud the main ideas in the mathematical formulation. The extension to other modes poses no serious difficulty, although the algebra is more cumbersome.

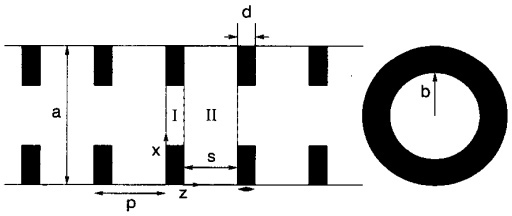

Fig. 1 *Cross-section and side view of corrugated circular waveguide*

2 Theory

We focus on the structure shown in Fig. 1. It consists of a circular waveguide of radius a, periodically loaded with irises of thickness d and inner radius b. The period

IEE Proceedings online no. 19990140

DOI: 10.1049/ip-map:19990140

Paper first received 26th February 1998 and in revised form 8th September 1998

S. Amari and R. Vahldieck are with the Laboratory for Field Theory and Microwave Electronics, Swiss Federal Institute of Technology, ETH–Zentrum, 8092 Zürich, Switzerland

J. Bornemann is with the Laboratory for Lightwave Electronics, Microwaves and Communications (LLiMiC), Department of Electrical and Computer Engineering, University of Victoria, Victoria, BC, Canada

of the structure is p. Owing to the periodicity of the structure, it is sufficient to analyse only one unit cell. The connection between adjacent cells is provided by the Floquet condition, which we write in the form [8]

$$f(z+p) = e^{-\theta p} f(z), \quad \forall z \tag{1}$$

Here $f(z)$ is a generic component of the electromagnetic field and θ is the propagation constant of the mode.

The unit cell is subdivided into two distinct regions, as shown in Fig. 1. Let the transverse electric field at $z = 0$, $z = d$ and $z = p$ be denoted by $X_1(x)$, $X_2(x)$ and $X_3(x)$, respectively. The Floquet condition is included in the theory from the outset by requiring the following relation

$$X_3(x) = e^{-\theta p} X_1(x) \tag{2}$$

Following our previous approach [9], we derive two coupled integral equations for the two remaining functions $X_1(x)$ and $X_2(x)$. Starting from the modal expansions of E_ϕ in both regions, the modal expansion coefficients are eliminated in favour of the functions X_1 and X_2. Enforcing the continuity of H_ρ at $z = d$ and its periodicity at $z = p$, we obtain two coupled integral equations:

$$\sum_{n=1}^{\infty} Y_n^{II} g_n^{II} \frac{\tilde{X}_2^{II}(n)\cos(k_{zn}^{II}S) - e^{-\theta p}\tilde{X}_1^{II}(n)}{\sin(k_{zn}^{II}S)} J_1\left(x_{n1}\frac{\rho}{a}\right) = \sum_{n=1}^{\infty} Y_n^{I} g_n^{I} \frac{\tilde{X}_1^{I}(n) - \cos(k_{zn}^{I}d)\tilde{X}_2^{I}(n)}{\sin(k_{zn}^{I}d)} J_1\left(x_{n1}\frac{\rho}{b}\right) \qquad 0 \le \rho \le b \tag{3}$$

and

$$\sum_{n=1}^{\infty} Y_n^{II} g_n^{II} \frac{\tilde{X}_2^{II}(n)e^{\theta p} - \cos(k_{zn}^{II}S)\tilde{X}_1^{II}(n)}{\sin(k_{zn}^{II}S)} J_1\left(x_{n1}\frac{\rho}{a}\right) = \sum_{n=1}^{\infty} Y_n^{I} g_n^{I} \frac{\tilde{X}_1^{I}(n)\cos(k_{zn}^{I}d) - \tilde{X}_2^{I}(n)}{\sin(k_{zn}^{I}d)} J_1\left(x_{n1}\frac{\rho}{b}\right) \qquad 0 \le \rho \le b \tag{4}$$

Here J_1 is the Bessel function of order one and x_{n1} is its root of order n. The modal propagation constants are given by

$$k_{zn}^{I} = \sqrt{k_0^2 - \left(\frac{x_{n1}}{b}\right)^2}, \quad k_0 = \omega\sqrt{\mu_0\epsilon_0}$$
$$k_{zn}^{II} = \sqrt{k_0^2 - \left(\frac{x_{n1}}{a}\right)^2} \tag{5}$$

The wave admittances are related to the modal propagation constants through $Y_n^i = k_{zn}^i/\omega\mu_0$, where ω is the angular frequency.

The spectra of the functions $X_1(x)$ and $X_2(x)$ over the modes of the two regions are defined by

$$\tilde{X}_i^{I}(n) = g_n^{I} \int_0^b \rho d\rho X_i(\rho) J_1\left(x_{n1}\frac{\rho}{b}\right) \tag{6}$$

$$\tilde{X}_i^{II}(n) = g_n^{II} \int_0^b \rho d\rho X_i(\rho) J_1\left(x_{n1}\frac{\rho}{a}\right) \tag{7}$$

The normalisation constants g_n^I and g_n^{II} are given by

$$g_n^{I} = \frac{\sqrt{2}}{b|J_1'(x_{n1})|} \tag{8}$$

$$g_n^{II} = \frac{\sqrt{2}}{a|J_1'(x_{n1})|} \tag{9}$$

To solve the integral equations, the functions $X_1(x)$ and $X_2(x)$ are expanded in series of basis functions of the form

$$X_1(x) = \sum_{i=1}^{M} u_i B_i(x) \tag{10}$$

$$X_2(x) = \sum_{i=1}^{M} v_i B_i(x) \tag{11}$$

The same set of basis functions is used at both discontinuities since they have identical geometries. Applying Galerkin's method [12], we obtain two sets of matrix equations in [**u**] and [**v**]:

$$\begin{bmatrix} \mathbf{A} & \mathbf{C} \\ \mathbf{C} & \mathbf{A} \end{bmatrix} \begin{bmatrix} \mathbf{u} \\ \mathbf{v} \end{bmatrix} + \begin{bmatrix} \mathbf{D}e^{-\theta p} & 0 \\ 0 & \mathbf{D}e^{\theta p} \end{bmatrix} \begin{bmatrix} \mathbf{u} \\ \mathbf{v} \end{bmatrix} = 0 \tag{12}$$

where θ is the unkown propagation constant. The entries of the matrices in eqn. 12 are given by

$$A_{ij} = \sum_{n=1}^{\infty} Y_n^{I} \frac{\tilde{B}_i^{I}(n)\tilde{B}_j^{I}(n)}{\sin(k_{zn}^{I}d)} \tag{13}$$

$$C_{ij} = -\sum_{n=1}^{\infty} Y_n^{II} \frac{\tilde{B}_i^{II}(n)\tilde{B}_j^{II}(n)}{\tan(k_{zn}^{II}S)} - \sum_{n=1}^{\infty} Y_n^{I} \frac{\tilde{B}_i^{I}(n)\tilde{B}_j^{I}(n)}{\tan(k_{zn}^{I}d)} \tag{14}$$

and

$$D_{ij} = \sum_{n=1}^{\infty} Y_n^{II} \frac{\tilde{B}_i^{II}(n)\tilde{B}_j^{II}(n)}{\sin(k_{zn}^{II}S)} \tag{15}$$

Eqn. 12 is not in a convenient form because of the appearance of two different functions of θ, i.e. $e^{\theta p}$ and $e^{-\theta p}$. A direct solution requires finding the roots of a nonlinear determinant equation; an approach we want to avoid. We first eliminate the vector [**v**] to obtain a reduced equation in terms of [**u**] only, or

$$[\mathbf{R}][\mathbf{u}] + [\mathbf{U}][\mathbf{u}]e^{\theta p} + [\mathbf{U}]^t[\mathbf{u}]e^{-\theta p} = 0 \tag{16}$$

The matrices in eqn. 16 are given by

$$[\mathbf{R}] = AC^{-1}A + DC^{-1}D - C \tag{17}$$

and

$$[\mathbf{U}] = AC^{-1}D, \quad [\mathbf{U}]^t = DC^{-1}A \tag{18}$$

Let $\lambda = e^{\theta p}$ and note that $e^{-\theta p} = 1/\lambda$. We then have the following eigenvalue problem:

$$[\mathbf{U}]^{-1}[\mathbf{R}]\lambda[\mathbf{u}] + \lambda^2[\mathbf{u}] + [\mathbf{U}]^{-1}[\mathbf{U}]^t[\mathbf{u}] = 0 \tag{19}$$

Let us introduce a vector [**w**] of the same dimension as [**u**] such that

$$[\mathbf{w}] = \lambda[\mathbf{u}] \tag{20}$$

The eigenvalue equation can finally be rewritten in the more convenient form

$$\begin{bmatrix} \mathbf{U}^{-1}\mathbf{R} & \mathbf{U}^{-1}\mathbf{U}^t \\ -\mathbf{I} & 0 \end{bmatrix} \begin{bmatrix} \mathbf{w} \\ \mathbf{u} \end{bmatrix} + \lambda \begin{bmatrix} \mathbf{w} \\ \mathbf{u} \end{bmatrix} = 0 \tag{21}$$

Here $\mathbf{I}$ is the identity matrix of order $\mathbf{M} \times \mathbf{M}$. Eqn. 21 shows explicitly that the propagation constants of the Floquet modes are determined from the classical eigenvalues of a real matrix. The large repertoire of commercial software packages can be used to solve it.

To complete the numerical solution, appropriate basis functions are needed. As an iris of finite thickness has a metallic wedge of internal angle 90°, at whose vicinity the tangential electric field vanishes as $r^{2/3}$ when

$r \to 0$ [8], we use the following basis functions obtained using a weighting factor similar to that of Kitazawa *et al.* [10]:

$$B_i(\rho) = \frac{J_1(x_{i1}\frac{\rho}{b})}{(1-(\frac{\rho}{b})^2)^{1/3}}, \quad i = 1, 2, \ldots \qquad (22)$$

The spectra of these basis functions over the modes of the two sections of the waveguide are computed numerically.

Note that the case of zero-thickness irises is best solved directly instead of from taking the limit $d \to 0$. Since the discussion is similar to the analysis above, it is not presented here. There are, however, multiple reflections taking place between the faces of the irises; the $k_0 - \beta$ diagram (Fig. 4) is more complex for thick irises.

3 Numerical results and discussion

To validate the approach and the computer code, we computed the propagation constants of the first few TE_{0n} modes for the structure analysed by Clarricoats and Olver [1] when $b/a = 0.8$. Only the propagating modes with $\theta = j\beta$ are shown here. Since the value of the period is unfortunately not given by Clarricoats and Olver, we found that their results for TE_{01} and TE_{02} [[1], Figure 3.3, p. 26], agree very well with our results when the period is $p = a/5$ within the zero-thickness approximation. A computer code was written to solve the zero-thickness approximation directly and is available to interested readers.

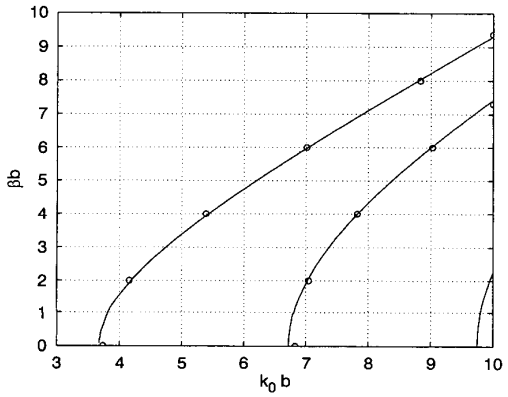

Fig. 2 *Propagation constant of first three TE_{0n} modes as a function of k_0b obtained from three basis functions when $a = 19.5$mm, $p = a/5$ and $b/a = 0.8$*
——— our approach
◦ Clarricoats and Olver's approach [1]

Fig. 2 shows a plot of the propagation constant βb as a function of $k_0 b$. The agreement is excellent within the readability of the quoted results. These results were obtained using three basis functions, and the sums in the entries of the matrices needed 30 terms to reach convergence. The additional mode which starts at $k_0 b = 9.8$ was not reported previously [1].

The first branch of the TE_{01} mode was also determined when the thickness of the irises is non-zero. Fig. 3 shows the results obtained from the present approach with three basis functions for the same dimensions as reported by Davies and Goldsmith [13]. The experimental results [13] are in excellent agreement with our computed results.

We also carried out numerical experiments in the limits $d \to p$ and $b \to a$ and obtained excellent agreement between the numerical results and the limiting analytical results.

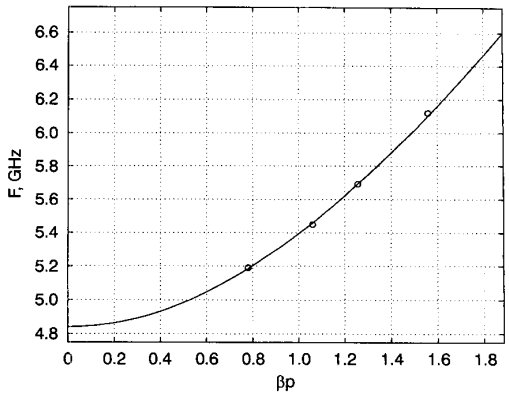

Fig. 3 *Dispersion curve of TE_{01} mode obtained from three basis functions when $2a = 7.9423$cm, $p = 2$cm, $2b = 7.112$cm and $d = 0.2449$cm*
◦ experimental results [8].

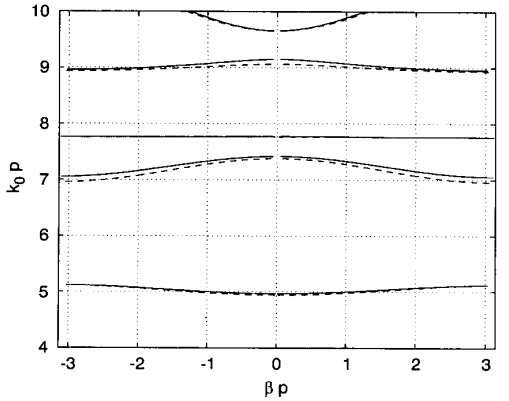

Fig. 4 *$k_0 - \beta$ obtained from three basis functions when $a = 19.5$mm, $p = a$, $b = a/2$ and $d = a/10$ (———)*
(– – –) dispersion diagram of Fig. 5 for same dimensions

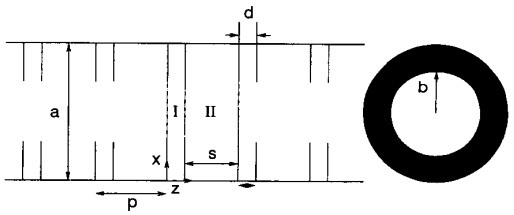

Fig. 5 *'Equivalent' of Fig. 1 where each thick iris is replaced with two irises of zero-thickness*

Fig. 4 shows the entire $k_0 - \beta$ diagram when $p = a$, $b = a/2$ and $d = a/10$. The solid lines represent the dispersion diagram of the structure with thick irises. To show the effect of multiple reflections, reflections between the two sides of the corrugations at $z = 0$ and $z = d$, we also plotted the diagram of a structure where each thick iris is replaced with two infinitely thin irises separated by a distance d (dashed lines) (Fig. 5). The agreement between the two diagrams clearly suggests that the physics of the problem is dominated by the discontinuities at the faces of the iris. The basis functions for the zero-thickness approximation were obtained using a weighting factor similar to the basis functions used by Kitazawa *et al.* [10], but with Bessel functions replacing the polynomials. The data for Fig. 4 were calculated using three basis functions and

30 terms in the sums appearing in entries of the matrices in eqns. 13–15. The presence of the band-gaps in the $k_0 - \beta$ diagram is evident. Note that other modes may be present in the frequency range where the TE_{0n} modes are not propagating. A much more exhaustive investigation of the spectrum of a corrugated circular waveguide has been carried out by Clarricoats and Olver [1].

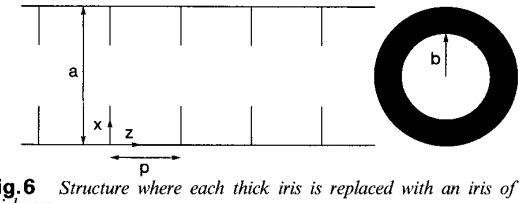

Fig. 6 *Structure where each thick iris is replaced with an iris of zero thickness*

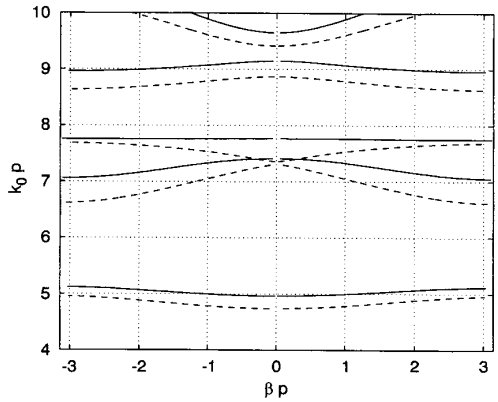

Fig. 7 *$k_0 - \beta$ diagram of Fig. 1 (———) and Fig. 6 (– – –) when a = 19.5mm, $p = a$, $b = 0.5a$ and $d = a/10$ (in Fig. 1)*
Compare Figs. 4 and 7

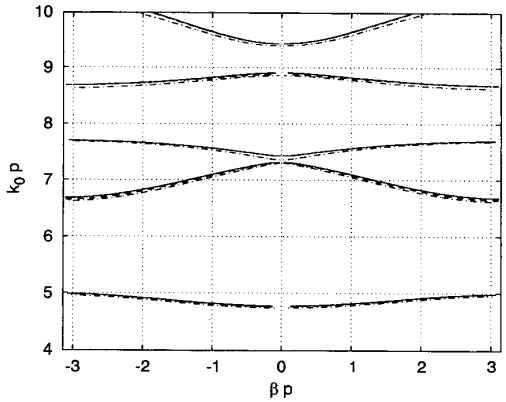

Fig. 8 *$k_0 - \beta$ diagram of Fig. 1 (———), Fig. 5 (– – –) and Fig. 6 (– · –) when a = 19.5mm, $p = a$, $b = 0.5a$ and $d = a/50$*
The three structures are practically equivalent for these dimensions and this frequency range

To further investigate the accuracy of the zero-thickness approximation, we computed the dispersion diagram of a structure of the same period and where each thick iris is replaced by only one zero-thickness iris (Fig. 6). Fig. 7 shows the dispersion diagram when $p = a$, $b = a/2$ and $d = a/10$ (solid line) and the dispersion diagram of Fig. 6 (dashed lines) for the same period and ratio b/a. By comparing Figs. 4 and 7, it is obvious that, at least for this value of d, replacing the thick iris by two infinitely thin irises (Fig. 5) is a better approximation than replacing it with a single iris of zero thickness (Fig. 6). This again emphasises the importance of multiple reflections in the unit cell; there are two discontinuities per unit cell, whereas Fig. 6 has only one. Obviously, the two approximations should both be adequate in the limit $d \to 0$. This is clearly shown in Fig. 8, where $p = a$, $b/a = 0.5$ and $d = a/50$. The solid lines are the dispersion diagram with the thickness accurately taken into account, the dashed lines are those of Fig. 5 and the dotted-dashed lines are those of Fig. 6. The agreement between the three results is good and becomes even better for smaller values of d.

There is, however, an important difference between Figs. 5 and 6 due to the presence of two discontinuities per unit cell. This leads to a splitting in the dispersion diagram. For the particular case where the two irises are separated by a distance $d = p/2$, the dispersion diagram should fold back on itself; this is shown in Fig. 10.

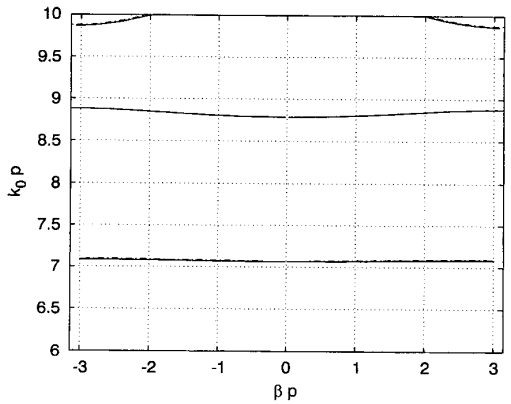

Fig. 9 *Convergence of $k_0 - \beta$ diagram when a = 19.5mm, $p = a$, $b = 0.4a$ and $d = p/2$*
One (– · –), two (– –) and three (——) basis functions

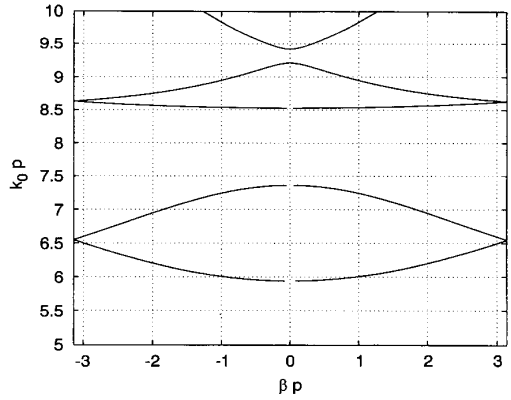

Fig. 10 *$k_0 - \beta$ diagram of Fig. 5 when a = 19.5mm, $p = a$, $b = 0.5a$ and $d = p/2$*
Note that two branches terminate at same point $\beta p = \pm\pi$

The convergence of the numerical solution was also investigated. Fig. 9 shows the dispersion diagram when $p = a$, $b = 0.4a$ and $d = p/2$ when one, two, and three basis functions are used. It is evident that the TE_{01} mode is accurately determined with only one basis function. All the modes propagating in the frequency range in Fig. 9 are accurately determined using, at most, three basis functions.

An additional test of the approach consists of determining the dispersion diagram of Fig. 6 when the infinitely thin irises are separated by a distance of $p/2$. In

this case, the period is actually $p/2$ and the dispersion diagram should reflect this property. In particular, at the edge of the Brillouin zone, at least two branches must meet. This is clearly shown in Fig. 10, where there is no gap at ($\beta p = \pm\pi$, $k_0 p = 6.55$) and ($\beta p = \pm\pi$, $k_0 p = 8.63$). This provides an additional validation of the approach. Further discussion of dispersion diagrams of periodic structures can be found elsewhere [14].

4 Conclusions

We have presented an accurate field theoretical analysis of the dispersion properties of circular waveguides periodically loaded with irises of finite thickness. The propagation constants of the Floquet modes are determined from the classical eigenvalues of a characteristic matrix instead of a nonlinear determinant equation. Although only TE_{0n} modes have been analysed, the technique is applicable to other TE, TM and hybrid modes of a periodically loaded circular waveguide.

5 References

1 CLARRICOATS, P.J.B., and OLVER, A.D.: 'Corrugated horns for microwave antennas' (Peter Peregrinus, London, UK, 1984)

2 CLARRICOATS, P.J.B., and SOBHY, M.I.: 'Propagation behaviour of periodically loaded waveguides', *Proc. Inst. Electron. Eng.*, 1968, **115**, pp. 652–661

3 BRYANT, G.H.: 'Propagation in corrugated waveguides', *Proc. Inst. Electr. Eng.*, 1969, **116S**, pp. 203–213

4 JAMES, G.L.: 'Analysis and design of TE_{11}-to-HE_{11} corrugated cylindrical waveguide mode converters using ring loaded slots', *IEEE Trans., Microwave Theory Technol.*, 1981, **29**, pp. 1059–1066

5 CLARRICOATS, P.J.B., and SAHA, P.K.: 'Propagation and radiation behaviour of corrugated feeds', *Proc. Inst. Electr. Eng.*, 1971, **118**, pp. 1167–1176

6 MITTRA, R., and LEE, S.: 'Analytical techniques in the theory of guided waves' (MacMillan, New York, 1974)

7 NAVARRO, M.S., ROZZI, T.E., and LO, Y.T.: 'Propagation in a rectangular waveguide periodically loaded with resonant irises', *IEEE Trans., Microwave Theory Technol.*, 1980, **28**, pp. 857–865

8 COLLIN, R.E.: 'Field theory of guided waves' (IEEE Press, New York, 1991)

9 AMARI, S., BORNEMANN, J., and VAHLDIECK, R.: 'Accurate analysis of scattering from multiple waveguide discontinuities using the coupled-integral-equations technique', *J. Electromag. Waves Appl.*, 1996, **10**, pp. 1623–1644

10 KITAZAWA, T., HAYASHI, Y., and SUZUKI, M.: 'Analysis of the dispersion characteristics of slot line with thick metal coating', *IEEE Trans., Microwave Theory Technol.*, 1980, **28**, pp. 387–392

11 KITAZAWA, T., and ITOH, T.: 'Propagation characteristics of coplanar-type transmission lines with lossy media', *IEEE Trans., Microwave Theory Technol.*, 1991, **39**, pp. 1694–1700

12 HARRINGTON, R.F.: 'Field computation by moment methods' (Krieger, Malabar, Florida, 1987)

13 DAVIES, J.B., and GOLDSMITH, B.J.: 'An analysis of general mode propagation and the pulse-shortening phenomenon in electron linear accelerators', *Philips Res. Reports.*, 1968, **23**, pp. 207–232

14 BRILLOUIN, L.: 'Propagation in periodic structures' (Dover, New York, 1953)